

# APPLICATION OF CFD TECHNOLOGY IN WIND TURBINE ICING PROBER DESIGN

Yi Xian(易贤), Chen Kun(陈坤), Wang Kaichun(王开春), Ma Honglin(马洪林)

(State Key Laboratory of Aerodynamics, China Aerodynamics Research  
and Development Center, Mianyang, 621000, P. R. China)

**Abstract:** A series of numerical methods, which are suitable to design the shape and configuration of the icing prober for the horizontal axis wind turbine, are presented. The methods are composed of a multiple reference frame (MRF) method for calculating flow field of air, a Lagrangian method for computing droplet trajectories, an Eulerian method for calculating droplet collection efficiency, and an arithmetic for fast computing ice accretion. All the numerical methods are based on the computational fluid dynamics (CFD) technology. After proposing the basic steps and ideas for the design of the icing detection system, the shape and configuration of the icing prober for a 1.5 MW horizontal axis wind turbine are then obtained with the methods. The results show that the numerical methods are efficient and the CFD technology plays an important role in the design process.

**Key words:** wind turbine; ice accretion; computational fluid dynamics; icing detection; aerodynamic characteristics

**CLC number:** TK83

**Document code:** A

**Article ID:** 1005-1120(2013)03-0264-05

## INTRODUCTION

When a wind turbine works in cold climate and meets rain and snow or clouds containing supercooled droplets, ice accretion may occur on the surface of the wind turbine components such as blades, hub and engine room. Icing may have undesirable effects on wind turbine performance<sup>[1-2]</sup>. Ice on the blade can change the shape of blade, degrade the aerodynamic characteristics, decrease the torque, and reduce the wind-energy utilization coefficient and the output power. Former study shows that a light icing event can produce enough surface roughness to considerably reduce aerodynamic efficiency. Furthermore, the presence of ice on various structures also results in vibration, which causes added stress on the components and increases the fatigue of unit components. Wind turbines may stop rotating or collapse due to severe icing. Sometimes, the ice block will drop or throw out and bring an unexpected injury and damage. Since ice can only be found and esti-

mated by the eyes of workers in most cases, it is difficult to know the details about ice on the wind turbine. As a result, it is necessary to develop ice protection technology.

Different types of icing on structures can occur<sup>[3]</sup>. The major two are precipitation icing and in-cloud icing. Precipitation icing takes place as a result of freezing rain (or drizzle) or accumulation of wet snow. In-cloud icing occurs when the structures considered are inside clouds which contains supercooled water droplets. Since the in-cloud icing is a familiar sight in practice, we have been making efforts to develop the approach to designing in-cloud icing detection system for wind turbine. In this paper, a series of numerical methods, which are based on the computational fluid dynamics (CFD) technology, are presented. The process and results of designing shape and configuration of an icing prober with the numerical methods are demonstrated.

## 1 NUMERICAL METHOD

The numerical methods are composed of a

**Received date:** 2013-04-10; **revision received date:** 2013-07-11

**Corresponding author:** Yi Xian, Associate Researcher, Ph. D., E-mail: yixian-2000@163.com.

multiple reference frame (MRF) method for calculating air flowfield around the wind turbine, a Lagrangian method for computing droplet trajectories in the field, an Eulerian method for calculating droplet collection efficiency, and an arithmetic for fast computing ice accretion.

### 1.1 Calculation method for flowfield

To design configuration and shape of the icing prober, air flow field around the wind turbine must be obtained. There are many methods for wind turbine flow field calculation<sup>[4-5]</sup>. In this paper, the MRF method is used to calculate air flow. The governing equations in both rotational and inertia frame can be written in the following transport form<sup>[6]</sup>

$$\frac{\partial(\rho_a \varphi)}{\partial t} + \nabla \cdot (\rho_a \mathbf{u}_a \varphi - \Gamma_\varphi \text{grad} \varphi) = q_\varphi \quad (1)$$

where  $\rho_a$  is the air density,  $\mathbf{u}_a$  the air velocity relative to the frame and  $q_\varphi$  the source term. When  $\varphi$ ,  $\Gamma_\varphi$  and  $q_\varphi$  are given different physical values, Eq. (1) can represent different kinds of equation, such as continuum, momentum and energy equation. A finite-volume method which is described in detail in Ref. [6] is used to solve Eq. (1).

### 1.2 Calculation method for droplet trajectory

In order to determine where to place the ice detection system, it is necessary to know droplet trajectory around the wind turbine. A Lagrangian method is employed to calculate droplet trajectory. The droplet movement equation is<sup>[7]</sup>

$$\frac{d^2 \mathbf{x}}{dt^2} = \left( \frac{C_d Re}{24} \right) \frac{1}{K_a} (\mathbf{u}_d - \mathbf{u}_a) + K_b \mathbf{g} \quad (2)$$

where

$$K_a = \frac{1}{18} \frac{\rho_d}{\mu} d_{eq} \quad (3)$$

$$K_b = \frac{\rho_d - \rho_a}{\rho_d} \quad (4)$$

In Eqs. (2–4),  $x$  is the droplet position,  $\mathbf{g}$  the acceleration of gravity,  $C_d$  the drag coefficient,  $Re$  the relative Reynolds number,  $\mathbf{u}_a$  the air velocity,  $\mathbf{u}_d$  the droplet velocity,  $\rho_a$  the air density,  $\rho_d$  the water droplet density,  $d_{eq}$  the droplet diameter, and  $\mu$  the viscous coefficient of air. Eq. (2) is

solved with the 1st Euler scheme<sup>[7]</sup>.

### 1.3 Calculation method for droplet collection efficiency

The collection efficiency on the structure surface is computed based on the distribution of air field with an Eulerian method<sup>[6]</sup>. The governing equations of the water phase are composed of continuum and momentum equations, shown as

$$\frac{\partial(\rho_d \alpha)}{\partial t} + \nabla \cdot (\rho_d \alpha \mathbf{u}_d) = 0 \quad (5)$$

$$\frac{\partial(\rho_d \alpha \mathbf{u}_d)}{\partial t} + \nabla \cdot (\rho_d \alpha \mathbf{u}_d \mathbf{u}_d) = \rho_d \alpha K (\mathbf{u}_a - \mathbf{u}_d) + \rho_d \alpha \mathbf{g} \quad (6)$$

where  $\alpha$  is the droplet volume fraction, and  $K$  the called inertia factor. Eqs. (5–6) can also be written in the form of transport equation

$$\frac{\partial(\rho_d \alpha \varphi)}{\partial t} + \nabla \cdot (\rho_d \alpha \mathbf{u}_d \varphi) = q_\varphi \quad (7)$$

When  $\varphi$  is equal to 1,  $\mathbf{u}_d$ ,  $\mathbf{v}_d$  and  $\mathbf{w}_d$  respectively, Eq. (7) is called continuum equation and momentum equation in  $x$ ,  $y$ ,  $z$  directions respectively.

In order to obtain water collection efficiency and impingement characteristics, the same numerical method with air field calculation is used to discrete and solve Eq. (7). The droplet volume fraction,  $\alpha$ , can be obtained after the equation is solved. The droplet collection efficiency,  $\beta$ , which shows the distribution of liquid water on structure surface, can be calculated as

$$\beta = \frac{\alpha}{\alpha_\infty} \frac{|\mathbf{u}_d \cdot \mathbf{n}|}{|\mathbf{u}_\infty|} \quad (8)$$

where  $\alpha_\infty$  and  $\mathbf{u}_\infty$  are the droplet volume fraction and air velocity of far field, and  $\mathbf{n}$  is the unit vector normal to body surface.

### 1.4 Fast calculation method for ice accretion

To obtain the relation between prober icing and wind turbine icing, the method for fast computing ice accretion is necessary. The following formula is used to compute ice thickness<sup>[8]</sup>.

$$h = \frac{f \cdot \beta \cdot \text{LWC} \cdot V \cdot dt}{\rho_i} \quad (9)$$

where  $f$  is the fraction of freeze, and  $0 \leq f \leq 1$ , LWC the liquid water content in the atmosphere,  $V$  the air velocity in far field,  $dt$  the icing time,

and  $\rho_i$  the density of ice. In Eq. (9),  $f$  is given the value of 1 usually, and LWC,  $V$ ,  $dt$  and  $\rho_i$  are input conditions, which are specified by designer.

## 2 BASIC STEPS OF ICE DETECTION SYSTEM DESIGN

A approach to designing ice detection system for wind turbine has been proposed<sup>[9]</sup>. The main idea of the approach is to integrate icing sensors on an extra prober and to predict ice on wind turbine according to the prober icing. The approach can be divided into following five steps. First, build numerical method for design based on the CFD method. Second, develop the advanced ice sensors according to the optical property of ice. Third, design the configuration and aerodynamic shape of the prober to assemble the ice sensor. Then the relationship between wind turbine icing and prober icing can be analyzed by numerical calculation, based on which, we can determine where the ice sensor should be installed on the surface of the prober. Fourth, calculate how icing affects the performance of wind turbine and then work out the alarm strategy. Finally, integrate the prober and the electronic system and form the whole ice detection system for wind turbine application. In above steps, the step 3 is the key step, which can be carried out only if the numerical method and tools have been developed.

## 3 DESIGN PROCESS AND RESULTS

### 3.1 Wind turbine configuration and frame

The authors of the paper have designed the shape and configuration of the icing prober for a 1.5 MW horizontal axis wind turbine. The radius of the turbine is 41 m. In the design process, the effects of tower are neglected. Multi-block structured mesh is generated. And there are  $18 \times 10^6$  grids. The wind turbine configuration and the frame are showed in Fig. 1. Fig. 2 shows the surface grid distributions near the hub.

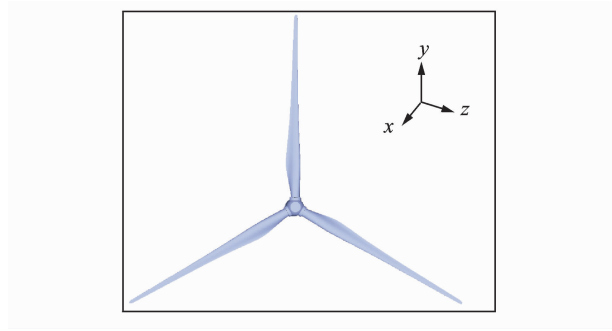


Fig. 1 Wind turbine configuration and frame

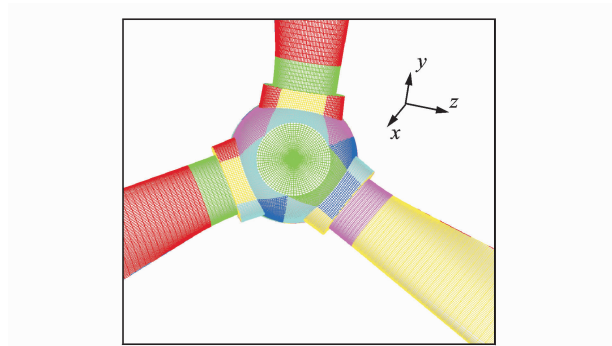


Fig. 2 Surface grids near hub

### 3.2 Air field around wind turbine

Firstly, air field about the wind turbine is calculated with the MRF method. Far field velocity is 11 m/s and the rotational speed is 17.4 r/min. Fig. 3 gives the contour of pressure relative to far field on the wind turbine surface. Typical streamlines around the wind turbine are given in Fig. 4, which shows that the streamlines keep the same direction with far field velocity before approaching the components. When close to body, streamlines deflect from old direction to the rotation direction of the turbine. More close to the turbine, more obvious the deflection is.

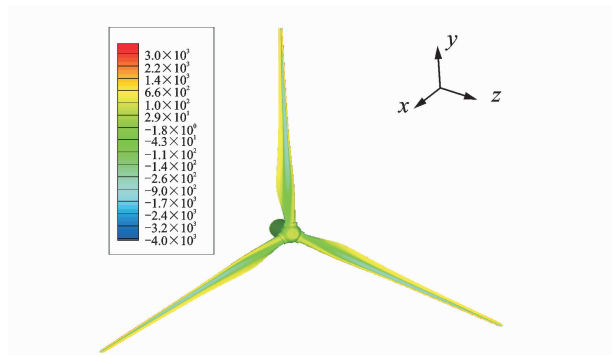


Fig. 3 Pressure distribution on blade

Behind the wind turbine plane, with the streamlines leaving the turbine, their orientation gradually turn back to the old direction. Above phenomena indicate that although rotation of turbine will bend the streamlines, the streamlines can always go back to their old direction.

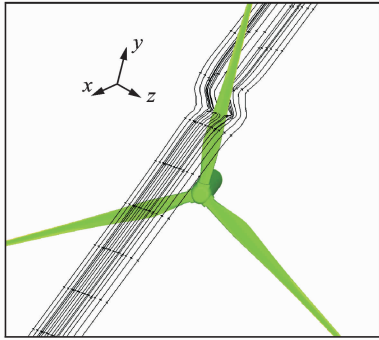


Fig. 4 Typical streamlines around wind turbine

### 3.3 Location for icing prober

The icing prober must be placed at a proper position so that the ice accretion can occur on the prober surface. To find the location for the icing prober, trajectories of water droplets are calculated after air field about the wind turbine is yielded. Fig. 5 shows typical trajectories of droplet with a diameter of  $100\ \mu\text{m}$ . It shows that only in the region very near the turbine, droplet trajectories deviate from streamlines due to inertia effect. In other space, the trajectories always accord with air streamlines.

The distribution of streamlines and trajectories reveals that rotation of blades cannot prevent water droplet going through the turbine plane. Since behind the turbine plane there is sufficient space on the shell of the engine room, the icing

prober can be placed there, which ensures not only ice can accrete on the prober, but also structures of the blades keep undamaged.

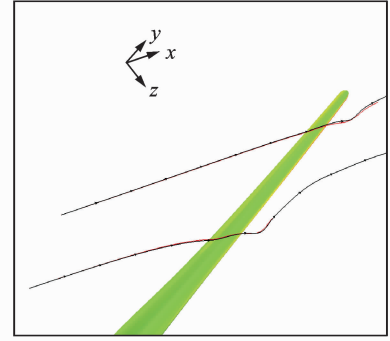


Fig. 5 Droplet trajectories and air streamlines

### 3.4 Design of prober configuration and shape

A prober with good configuration and shape can not only predict and reveal wind turbine icing but also be convenient for integrating and accommodating electronic system. Therefore a prober is proposed, showed in Fig. 6<sup>[9]</sup>. The prober is composed of four components. The first is the main component, which is an upright hollow wallboard with a columniform leading edge. This configuration can hold electronic system. The second is a half disk at the top of the wall. The third is a heave back behind the disk. The last component is a foundation with whorl holes. Fig. 6 also gives the numbering of the sensors. The circle signs on the prober surface are locations for placing sensors. We hope the combination of sensor 1 and sensor 2, the combination of sensor 3 and sensor 4 can reflect in-clouding icing on the middle part or tip of the blade, and sensor 5 can detect ice due to freezing rain.

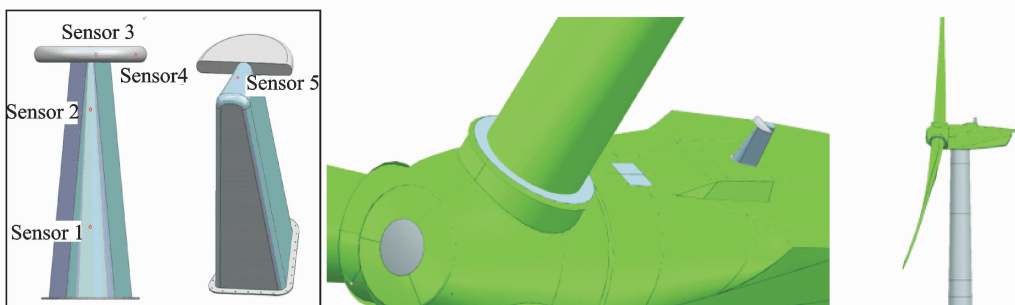


Fig. 6 Configuration of prober and sketch of wind turbine installed with prober

### 3.5 Validation of detection effects

A probe is effective only when the ice characteristics on blade can be predicted after obtaining the ice on the probe. To validate the detection effects, according to Eq. (9), water droplet collection efficiency on wind turbine and probe is needed.

Assuming  $\beta_1, \beta_2$  and  $\beta_3$  are the water droplet collection efficiency along the blade at position of  $r/R=97.6\%$ ,  $r/R=75.6\%$  and  $r/R=53.7\%$ . The collection efficiency at the positions of sensors 1—4 is  $\alpha_1, \alpha_2, \alpha_3$  and  $\alpha_4$  respectively. If ice accretion on sensor 1 and sensor 2 can indicate ice on middle position of blade and tip, and ice accretion on sensor 3 and sensor 4 can reveal ice on middle and outer position of the blade, we get

$$\beta_1/\beta_2 = \alpha_1/\alpha_2 \tag{10}$$

$$\beta_2/\beta_3 = \alpha_3/\alpha_4 \tag{11}$$

The numerical method described in section 1.3 is used to simulate characteristics of water droplet impingement to assess the detection effects. Far field velocity is 11 m/s, and the rotational speed is 17.4 r/min. The diameter of water

droplet for simulation is 20, 40, 100  $\mu\text{m}$ . Figs. 7—8 give collection efficiency of droplet with 40  $\mu\text{m}$  diameter on blade and probe respectively. The values of  $\beta_1, \beta_2, \beta_3, \alpha_1, \alpha_2, \alpha_3$  and  $\alpha_4$  are showed in Tables 1—2. The results show good agreement with Eqs. (10—11).

**Table 1 Droplet collection efficiency at positions of sensor 1 and sensor 2**

Droplet diameter/ $\mu\text{m}$	$\alpha_1$	$\beta_1/\beta_2$	$\alpha_2$ (ideal)	$\alpha_2$ (actual)
20	0.14	2.05	0.068	0.093
40	0.41	1.68	0.244	0.262
100	0.68	1.44	0.472	0.479

**Table 2 Droplet collection efficiency at positions of sensor 3 and sensor 4**

Droplet diameter/ $\mu\text{m}$	$\alpha_3$	$\beta_2/\beta_3$	$\alpha_4$ (ideal)	$\alpha_4$ (actual)
20	0.22	2.86	0.08	0.07
40	0.45	2.07	0.22	0.19
100	0.46	2.28	0.22	0.20

## 4 CONCLUSION

A series of numerical methods, which are based on CFD technology, are presented in the paper. The methods are adopted to design shape and configuration of the icing probe for a horizontal axis wind turbine. The process of design shows that CFD method plays an important role. The results indicate that the numerical methods are effective, which provide an efficient way to design icing probe and assess detection effects. All the conclusions are useful for future research.

### References:

[1] Jasinski W J, Noe S C, Selig M S, et al. Wind turbine performance under icing conditions[R]. AIAA-1997-0977, 1997.

[2] Zhu Chengxiang, Fu Bin, Sun Zhiguo, et al. Calculation of wind turbine anti\_icing heat load[J]. Journal of Nanjing University of Aeronautics & Astronautics, 2011, 43(5):701-706. (in Chinese)

[3] Frohboese P, Anders A. Effects of icing on wind turbine fatigue loads[J]. Journal of Physics: Conference Series, 2007, 75: 012061.

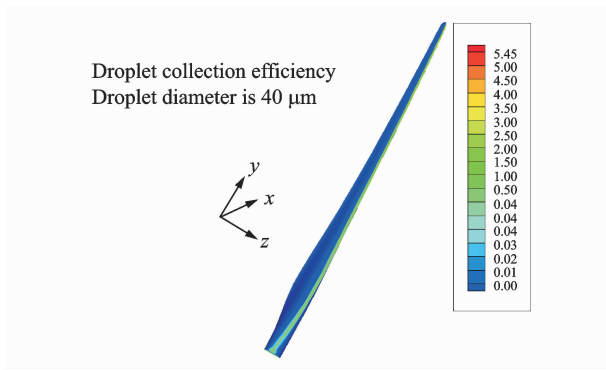


Fig. 7 Contour of collection efficiency on blade

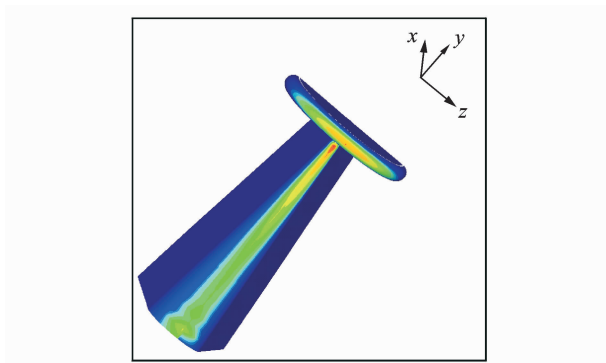


Fig. 8 Contour of collection efficiency on probe

- [4] Xu Bofeng, Wang Tongguang. Wind turbine aerodynamics performance prediction based on free-wake/panel model couple method[J]. Journal of Nanjing University of Aeronautics & Astronautics, 2011, 43(5):592-597. (in Chinese)
- [5] Zhong Wei, Wang Tongguang. Numerical analysis of the wind turbine blade-tip vortex[J]. Journal of Nanjing University of Aeronautics & Astronautics, 2011, 43(5):640-644. (in Chinese)
- [6] Yi Xian, Wang Kaichun, Gui Yewei, et al. Study on Eulerian method for icing collection efficiency computation and its application[J]. Acta Aerodynamic Sinica, 2010, 28(5):596-601. (in Chinese)
- [7] Yi Xian, Gui Yewei, Du Yanxia, et al. Study on the method of droplet diameter calibration in icing wind tunnel[J]. Journal of Experiments in Fluid Mechanics, 2010, 24(5):36-41,46. (in Chinese)
- [8] Yi Xian, Gui Yewei, Zhu Guolin. Study on the numerical method of a three-dimensional ice accretion model[J]. Acta Aeronautica et Astronautica Sinica, 2010, 31(11):2152-2158. (in Chinese)
- [9] Yi Xian, Zhao Ping, Chen Kun, et al. Design of icing prober for horizontal axis wind turbine[J]. Acta Aerodynamic Sinica, 2013, 31(2):260-265. (in Chinese)

(Executive editor: Zhang Huangqun)